Infrared absorption study of charge ordered $La_{0.5}Ca_{0.5-x}Sr_xMnO_3$ $(0.1 \leq x \leq 0.5)$ manganites

Indu Dhiman

Solid State Physics Division, Bhabha Atomic Research Centre, Mumbai - 400 085, India

A. Das

Solid State Physics Division, Bhabha Atomic Research Centre, Mumbai - 400 085, India

K. R. Priolkar

Department of Physics, Goa University, Taleigao Plateau, Goa - 403 206, India

P. S. R. Murthy

Department of Physics, Goa University, Taleigao Plateau, Goa - 403 206, India

Abstract

Infrared absorption study has been carried out on a series of half doped manganites, $La_{0.5}Ca_{0.5-x}Sr_xMnO_3$ $(0.1 \leq x \leq 0.5)$, with varying magnetic ground state. The charge ordering transition observed in samples with $x \leq 0.3$ is accompanied by a mode at $\sim 525cm^{-1}$ in addition to the stretching mode at $615cm^{-1}$ and bending mode at $400cm^{-1}$. Phonon hardening is found to occur below the CE - type antiferromagnetic ordering temperature. The value of the insulating gap decreases on doping with Sr from $727cm^{-1}$ to $615cm^{-1}$.

Keywords: Manganites, Charge ordering, Infrared

PACS: 61.12.Ld, 78.20.-e, 78.30.-j

1. Introduction

The correlation of magnetic and transport behavior in half doped $R_{0.5}A_{0.5}MnO_3$ (R: a trivalent earth ion, A: a divalent earth ion) manganites have lead to considerable research interest in these systems [1, 2, 3, 4]. Such correlated behavior in manganites has been explained by the interplay of double exchange and super exchange interactions coupled with strong electron - phonon interactions arising due to breathing and Jahn-Teller modes [5]. The Jahn-Teller distortion

Email address: adas@barc.gov.in (A. Das)

and double exchange interactions are competitive in nature. While the former tends to localize the charge in distortions of oxygen octahedra around Mn^{3+} ions, latter favors charge delocalization [6, 7]. As a consequence, the distortions of $Mn^{3+}O_6$ octahedra strongly influences the evolution of magnetic and structural phases. The infrared phonon spectra are sensitive to these local lattice distortions and its study sheds light on the important role played by MnO_6 vibrations, across metal-insulator transition [8].

The $LaMnO_3$ compound is an antiferromagnetic insulator having an orthorhombic structure in *Pnma* space group. The dominant Jahn-Teller effect arising from the presence of Mn^{3+} ions causes the structure to deviate from cubic to orthorhombic [9]. Infrared absorption study of this compound show 10 out of 25 lines predicted under orthorhombic symmetry [10]. In the mid infrared range this compound shows negligible absorption at all temperatures. Comparative analysis of measured spectra in association with lattice dynamical calculations allow reasonable assignment for the phonon modes observed in $LaMnO_3$ [11, 12]. Doping rare-earth with an alkaline earth metals like Ca, Sr, or Ba, in $R_{1-x}A_xMnO_3$ (A: alkaline earth metals) results in conversion of an appropriate number of Mn^{3+} to Mn^{4+} ions. This gives rise to ferromagnetic $Mn^{3+} - O - Mn^{4+}$ double exchange interactions whereby e_g electrons from Mn^{3+} is transferred to Mn^{4+} with a parallel spin configuration. The Ca doped $La_{1-x}Ca_xMnO_3$ manganites display a complex phase diagram as a function of doping (x) and temperature. Of particular interest are the half doped compounds which display coexisting ferromagnetic, antiferromagnetic, charge and orbital ordering as a function of temperature. The charge and orbital ordering in these systems is accompanied by a change in the sound velocity indicating a strong electron - acoustic phonon coupling [13]. The acoustic phonon frequency in this case is shown to be dependent upon the magnetic susceptibility in the antiferromagnetic state. This indicates a coupling between the phonons and magnetization which could be explored by infrared measurements. The Jahn - Teller mode, which plays an important role in the magnetism of hole doped manganites, is influenced by the optical phonon frequency [14]. Indeed, in the study of infrared spectra in $La_{1-x}Ca_xMnO_3$, it is found that the stretching modes progressively shifts from 596 to $588cm^{-1}$ on increasing Ca from $LaMnO_3$ to $CaMnO_3$ [15]. In another study, pressure dependent infrared studies on $La_{0.8}Ca_{0.2}MnO_3$ compound show the closing of optical gap with increasing pressure leading to metallization [16]. Kim et al. reported the external, bending, and stretching modes frequencies of MnO_6 octahedra in $La_{0.7}Ca_{0.3}MnO_3$

compound [8]. Infrared absorption studies have been reported for charge and orbitally ordered $La_{0.5}Ca_{0.5}MnO_3$ compound [17]. This compound exhibits ferromagnetic transition at $T_C \approx 225K$ and an antiferromagnetic transition at $T_N \approx 170K$, in addition to the transition from incommensurate to commensurate charge ordering in the antiferromagnetic region [18, 19]. The previously reported infrared absorption study in $La_{0.5}Ca_{0.5}MnO_3$ compound show the formation of an optical gap on lowering of temperature, leading to localization of the carriers [17]. As the screening action of the mobile holes weakens, phonon peaks become increasingly evident at lower temperature. However, the previous studies are inconclusive on the variation of infrared active modes in half doped compounds with varying magnetic ground states.

In the present study, we have made an attempt to understand the correlated variations in the infrared active modes of vibration of MnO_6 octahedra in association with polaronic absorption background, in charge and orbitally ordered systems. Towards this, temperature dependent infrared absorption spectroscopy study in $La_{0.5}Ca_{0.5-x}Sr_xMnO_3$ ($0.1 \leq x \leq 0.5$) manganites has been carried out. Previously reported neutron diffraction studies on these compounds show that with Sr doping, the CE – type antiferromagnetic structure is stable for x $<$ 0.3. At x = 0.3, CE – type ordering coexists with an A – type antiferromagnetic phase. At x = 0.4, A – type antiferromagnetic order replaces the CE – type state, in addition with the evidence of long range ferromagnetic ordering in the temperature range of 180 – 250K. All the compounds with $x \leq 0.4$ exhibit an insulating behavior. In x = 0.5 composition, long range ferromagnetic metallic phase is observed at temperatures below 310K [20, 21]. Pressure dependent neutron diffraction studies in these compounds show the equivalence of increasing $< r_A >$ and increasing external pressure in these compounds [22].

2. Experiment

The polycrystalline samples used for these measurements are the same on which neutron diffraction studies have been carried out and reported earlier [20]. Infrared measurements were performed using Shimadzu FTIR-8900 spectrophotometer at various temperatures below 300K in transmission mode in the range of 400 to 4000 cm^{-1}. Samples were mixed with KBr in the ratio of 1:100 by weight and pressed into pellets for infrared measurements. Temperature variation was achieved using an Oxford optical cryostat with KRS5 windows.

3. Results and Discussion

The structural and magnetic phase diagram of $La_{0.5}Ca_{0.5-x}Sr_xMnO_3$ ($0.1 \leq x \leq 0.5$) series obtained from unpolarized and polarized neutron diffraction study has been reported previously [20, 21]. The Sr-doped compounds in the $La_{0.5}Ca_{0.5-x}Sr_xMnO_3$ series with $x \leq 0.3$ are isostructural, possessing an orthorhombic distorted perovskite structure in *Pnma* space group at 300K. On lowering of temperature, these compounds exhibit transition to charge and orbital ordering at $T_{CO} \approx 225 - 250K$. The transition to a charge ordered state below T_{CO} is accompanied by a change of symmetry from orthorhombic structure in *Pnma* space group to monoclininc structure in $P2_1/m$ space group. The x = 0.4 sample crystallizes with two orthorhombic phases in the space group *Pnma* and *Fmmm*, whereas the end composition at x = 0.5 has a tetragonal structure in *I4/mcm* space group. Magnetically, with progressive increase in Sr doping, the CE – type antiferromagnetic phase is suppressed and ferromagnetic phase is favored. The CE – type antiferromagnetic phase is observed in x = 0.1 and 0.3 samples with antiferromagnetic transition temperatures as 175 and 150K, respectively. In x = 0.4, the CE – type antiferromagnetic structure is fully suppressed and A – type antiferromagnetic phase is observed with the transition temperature T_N = 200K. In addition, evidence of long range ferromagnetic ordering in the temperature range of 180 to 250K is observed only in x = 0.4 sample. Further increase in Sr doping to x = 0.5, the long range ordered ferromagnetic phase is established at all temperatures below 310K. In the present study we have selected few samples, such that each displays a different magnetic ground state.

The optical density ($O_d(\omega)$) in the infrared range between 400 and 1500cm^{-1} of $La_{0.5}Ca_{0.4}Sr_{0.1}MnO_3$ (x = 0.1) sample at temperatures between 100 and 300K is shown in figure 1. The optical density $O_d(\omega)$, which is proportional to the optical conductivity $\sigma(\omega)$, is defined as [23],

$$O_d(\omega) = ln[I_{KBr}(\omega)/I_s(\omega)] \propto \sigma(\omega)$$

where, $I_{KBr}(\omega)$ and $I_s(\omega)$ are the infrared intensities transmitted by a pure KBr pellets with and without the sample, at the same temperature, respectively. At 300K in x = 0.1 sample, two infrared absorption peaks at $\sim$ 400 and 600 cm^{-1} are observed. In *Pnma* space group there are 25 infrared active modes of vibrations, $9B_{1u}+7B_{2u}+9B_{3u}$. The infrared active phonon modes of symmetry B_{3u}, B_{2u}, and B_{1u} indicate toward the oscillations of dipole moment along the x, y,

and z directions, respectively. Additionally, there are $8A_u$ infrared silent modes and 3 acoustic modes as $B_{1u} + B_{2u} + B_{3u}$ [24]. In an infrared measurements on polycrystalline samples, the absorption spectra are broadened and therefore it is difficult to distinguish all the phonon modes as against measurements carried out on single crystal samples [25]. The infrared absorption peak evident at $\sim$ 400 and 600 cm^{-1} may be ascribed to the B_u symmetry bending and stretching mode, respectively [26]. According to Kim et al., bending mode is the motion of Mn and O ions located along a particular direction against the other oxygen ions in a plane perpendicular to the direction. While, the peak attributable to the stretching of Mn-O bonds corresponds to the internal motion of Mn ions against the oxygen octahedron and is sensitive to Mn-O bond lengths. At 300K, the infrared absorption peak at $\sim 600cm^{-1}$ is screened by a large background. Below 300K, the background is reduced and the absorption peak shows a strong temperature dependence, with built-up in intensity of stretching mode peak. Previously reported neutron diffraction results on these compounds show a large change in the apical and equatorial bond lengths, following the charge and orbitally ordered transition ($T_{CO} \approx 250K$) [20]. The difference between Mn-O bond lengths ($Mn - O_1$ along b axis (apical), $Mn - O_{21}$ and $Mn - O_{22}$ in ac plane (equatorial)) increases as temperature is reduced, which correlate with the stretching mode vibrations of $Mn - O$ bonds as described by Smirnova [24]. On lowering of temperature to 200K, an additional mode at $\sim 510cm^{-1}$ appears in the form of shoulder in main absorption peak and this becomes pronounced on reduction of temperature. This mode has been observed in other charge ordered manganites and has been identified with the structural transformation of orthorhombic structure in *Pnma* space group to charge and orbitally ordered monoclinic structure in $P2_1/m$ space group [17, 27, 24]. This behavior is in agreement with our previously reported neutron diffraction measurements on these samples, wherein the structural transformation from orthorhombic to charge and orbitally ordered monoclinic phase is observed while cooling. Contrastively, in compounds away from half doping, such as $La_{0.33}Ca_{0.67}MnO_3$ and $La_{0.67}Ca_{0.33}MnO_3$ systems, the *Pnma* space group is preserved down to lowest temperature, and shoulder like feature is absent in these samples, indicating that the mode at $510cm^{-1}$ arises due to the lowering of symmetry as a result of charge ordering [17, 28]. Further, on reducing temperature the absorption background is seen to deepen. According to Calvani et al. such gradual deepening of background with reducing temperature for $La_{0.5}Ca_{0.5}MnO_3$ compound provides an evidence for increasing localization of charge carriers [17]. This is

in agreement with the observation of sharp increase in resistivity below T_{CO} in Sr doped samples [20]. In contrast, the absorption background is seen to increase and the associated stretching mode at $590cm^{-1}$ is diminished in the ferromagnetically ordered $La_{0.67}Ca_{0.33}MnO_3$ system exhibiting an insulator to metal transition [28]. The infrared active mode at $190cm^{-1}$ ascribed to external mode was not observed in the present infrared study due to the limited range of instrument between 400 to $4000cm^{-1}$ [8]. The external mode at $190cm^{-1}$ represents a vibrating motion of the La (Ca) ions against the MnO_6 octahedra. In $La_{0.5}Ca_{0.2}Sr_{0.3}MnO_3$ (x = 0.3) sample with coexisting CE - and A - type antiferromagnetic ordering, the optical density ($O_d(\omega)$) shows similar temperature dependence between 100 and 300K, as observed in x = 0.1 sample. In x = 0.3 compound at 100K, the infrared absorption peak attributable to the stretching mode vibrations of MnO_6 octahedra is observed at $620cm^{-1}$ and is accompanied by a shoulder at $528cm^{-1}$, in association with the charge ordering transition. The increase in $< r_A >$ as a result of Sr doping leads to hardening of stretching mode.

Figure 2 displays frequency of stretching mode as a function of temperature in x = 0.1 and 0.3 samples. The frequencies are obtained by fitting the absorption curves to Lorentzian functions with the central frequency, half width and area under the peak as fitting parameters. At temperatures above the charge ordering transition a single Lorentzian function accounting for the stretching mode is used, while at low temperatures two Lorentzian functions assigned to stretching mode and the additional mode are used. It is observed that in both these samples a rapid shift in peak position is observed below 200K close to T_N. Around $T_{CO} \approx 250K$, no significant change is observed. This indicates coupling of the magnetic ordering with phonon modes. The temperature dependence of frequency of stretching mode in x = 0.3 sample displays behavior similar to x = 0.1 sample, as shown in figure 2. In x = 0.3 compound, above 250K, the estimation of frequency shift is difficult due to the significant broadening of the peak. The stretching mode vibration increases at the antiferromagnetic transition temperature T_N = 150K, as observed in x = 0.1 composition. Similar behavior of stretching mode frequency around the ferromagnetic transition and has been reported for $La_{0.67-x}Pr_xCa_{0.33}MnO_3$ compounds [29]. The stretching mode frequency at 100K increases from $\approx$615(1) cm^{-1} to 620(1)cm^{-1} with increase in x from 0.1 to 0.3, indicating the hardening of phonon mode. This is similar to the earlier reported observation of reduction in stretching mode frequency with increase in Ca substitution (with reducing $< r_A >$) in $La_{1-x}Ca_xMnO_3$

[15]. Theoretically, Lee and Min have examined the origin of phonon hardening (shifting of absorption peak to higher frequency below the ordering temperature) both in the charge ordered phase and the metallic phase of manganites. For charge ordered systems the study reveals that ordering of localized polarons is responsible for such a behavior [13, 14].

The insulating gap has been obtained by fitting the optical density $O_d(\omega)$, shown in figure 1, to the expression [17],

$$O_d(\omega) \propto [\omega - 2\triangle(T)]^{1/2} \tag{1}$$

for $\omega \geq 2\triangle(T)$, where $2\triangle(T)$ is the insulating gap. The fit to equation 1 for x = 0.1 sample is shown in figure 1 by dotted curves. The resulting values of $2\triangle(T)$ as a function of temperature for both heating and cooling cycles in x = 0.1 sample is shown in figure 3(a). As temperature is reduced the insulating gap increases, and reaches a stable value for $T \leq 150K$. The temperature at which insulating gap shows a sharp rise is identified with charge ordering transition temperature. This is in agreement with that reported from $\rho(T)$ studies. In addition, thermal hysteresis behavior in $2\triangle(T)$ for heating and cooling cycles is clearly discernible near the magnetic transition. This behavior arises due to the structural transition accompanying the antiferromagnetic transition, a characteristic feature occurring in $La_{0.5}Ca_{0.5}MnO_3$ system exhibiting CE-type antiferromagnetic state [17, 18]. For x = 0.1 sample, at 100K, the insulating gap is $\sim 727(1)cm^{-1}$. This value is in agreement with the previously reported infrared absorption study on $La_{0.5}Ca_{0.5}MnO_3$ compound yielding an insulating gap, $2\triangle(T) \approx 710cm^{-1}$ [17]. The variation of effective carrier numbers as a function of temperature, $n^*_{eff}(T)$, for x = 0.1 composition is shown in figure 3(b). This quantity is obtained by integration of optical density $O_d(\omega)$ over a suitable frequency range. The integration limits are the frequencies where $O_d(\omega)$ does not change appreciably with temperature. We have chosen $\omega_1 = 400cm^{-1}$ and $\omega_2 = 1500cm^{-1}$. In terms of optical density the expression for number of effective carriers $n^*_{eff}(T)$ is given as [17],

$$n^*_{eff}(T) = \int_{\omega_1}^{\omega_2} O_d(\omega)d\omega \propto n_{eff}(T) \tag{2}$$

As evident in figure 3(b) at low temperatures for large values of $2\triangle(T)$ (figure 3(a)), effective number of carriers are considerably reduced. Above 200K ($\sim T_{CO}$), the band gap starts reducing, which is consistent with an increasing

effective number of charge carriers. Besides, $n^*_{eff}(T)$ follows a thermal hysteresis behavior, similar to that evident in $2\triangle(T)$. Similar to x = 0.1 sample, from $O_d(\omega)$ data for x = 0.3 compound, $2\triangle(T)$ and $n^*_{eff}(T)$ are obtained. Figure 4 (a) and (b) shows temperature dependence of $2\triangle(T)$ and $n^*_{eff}(T)$ in x = 0.3 sample, respectively. Increase in $2\triangle(T)$ and correlated reduction in $n^*_{eff}(T)$ in x = 0.3 Sr doped sample on reducing temperature, similar to x = 0.1 composition, is in agreement with the previously reported transport studies [20]. Although, in comparison to x = 0.1 compound, the width of thermal hysteresis in $2\triangle(T)$ and $n^*_{eff}(T)$ is considerably reduced. Also, with increasing Sr doping, the value of $2\triangle(T)$ is reduced, which is in concurrence with weakening of charge ordered insulating state at higher Sr doping. Additionally, on lowering of temperature the absorption background is observed to decrease. Similar correlation between resistivity and $n^*_{eff}(T)$ has been observed in magnetically distinct compounds such as $La_{0.7}Ca_{0.3}MnO_3$ and $La_{0.75}Ca_{0.25}MnO_3$ [26, 30]. These compounds upon cooling near ferromagnetic transition temperature, show a transition from insulating to metallic state. Infrared study on these systems reveals a reduction in number of carriers with increasing temperature. There exists considerable disparity in the insulating band gap $2\triangle(T)$ for charge ordered manganites. Previous report on $La_{1-x}Ca_xMnO_3$ show that $2\triangle(T)$ values increase with x. At x = 0.5 compound, the gap is $\sim 0.45eV$ $(3600cm^{-1})$ [31]. Another study on $La_{0.5}Ca_{0.5}MnO_3$ reports the gap to be $320cm^{-1}$ [32]. However, in the $La_{5/8-y}Pr_yCa_{3/8}MnO_3$ system, where the charge ordering is known to be of $La_{0.5}Ca_{0.5}MnO_3$ type, the insulating gap is $\sim 0.38eV$ $(3065cm^{-1})$ [33].

The strength of electron - phonon coupling is related with the ratio given as, $2\triangle/k_BT_{CO}$ [34]. In x = 0.1 sample, the calculated value of $2\triangle/k_BT_{CO}$ is ≈ 4.8, which is reduced to 3.7 in x = 0.3 compound. This indicates that as Sr doping increases the strength of electron - phonon interaction is reduced. This suggests that enhanced electron - phonon coupling interaction may be important for stabilizing the charge ordered state. The obtained value of $2\triangle/k_BT_{CO}$ is in agreement with $La_{0.5}Ca_{0.5}MnO_3$ sample having value ≈ 4.8 [17]. Similar trend has been observed in $La_{1-x}Ca_xMnO_3$ as a function of Ca doping, wherein $2\triangle/k_BT_{CO}$ ratio is maximized for x = 0.50; therefore favoring the enhancement of charge ordered state [31]. However, according to this study the deduced ratio is of the order of $\approx$30 in x = 0.5 compound, which is much higher than the values reported here for Sr doped samples and previously reported study on $La_{0.5}Ca_{0.5}MnO_3$ [17].

At higher Sr doping in $La_{0.5}Ca_{0.1}Sr_{0.4}MnO_3$ (x = 0.4), neutron diffrac-

tion study carried out on this compound reveals that the antiferromagnetic spin structure changes from CE-type to A-type and consequently the nature of orbital ordering is modified[20, 21]. Further, transport measurements have shown that at low temperatures the resistivity of this compound is lowered as compared to the samples with $x \leq 0.3$ [20]. The infrared absorption spectra in x = 0.4 sample with A - type antiferromagnetic order, as shown in figure 5, is significantly different in comparison to samples with $x \leq 0.3$. While the typical Mn-O bond stretching mode with considerable weakening is still visible around $\sim 610 cm^{-1}$, the shoulder like feature observed in$x \leq 0.3$ samples is no longer visible in x = 0.4 sample. As discussed above, this feature has been ascribed to a transition to charge ordered state. Therefore, disappearance of this feature may be caused by the suppression of charge ordering in x = 0.4 compound. Similar behavior has been observed in compound exhibiting CE - and A - type antiferromagnetic ordering. The stretching and bending mode in the $Nd_{0.5}Sr_{0.5}MnO_3$ compound with CE - type antiferromagnetic ground state, exhibit splitting below T_N, which is in contrast with $Pr_{0.5}Sr_{0.5}MnO_3$ compound displaying A - type antiferromagnetic state. Nevertheless, the background attributed to localization of charge carriers still exhibits reduction while cooling from 300K. This implies decrease in the number of effective carriers with reducing temperature. However, the estimated value of $n^*_{eff}(T)$ using equation 2 exhibits a nearly linear temperature dependence, in contrast to compounds with $x \leq 0.3$. A fit to equation 1, as performed in $x \leq 0.3$ compounds, could not be carried out in x = 0.4 composition due to significant weakening of the stretching mode peak. Interestingly, in a previously reported optical conductivity measurements on single crystal of $Pr_{0.5}Sr_{0.5}MnO_3$ compound, having an A-type antiferromagnetic spin structure, the temperature dependence of spectral weight (measured by the variation of $n^*_{eff}(T)$) shows a strong correlation with the magnetic phase transition [35]. The infrared absorption measurements as a function of temperature were also performed in x = 0.5 composition, which display tetragonal crystal structure with *I4/mcm* space group and the long range ordered ferromagnetic state at all temperatures below 310K. A broad hump attributable to the presence of stretching mode at $\sim 600 - 620 cm^{-1}$ is observed, exhibiting no significant change as a function of temperature. Similar to samples with $x \leq 0.3$, the $n^*_{eff}(T)$ exhibits an increase with increasing temperature. This provides a signature of reduction in optical band gap with Sr doping, favoring delocalization of carriers. Therefore, in the present study we observe that position and intensity of the absorption peak is significantly affected as a function in Sr

doping in $La_{0.5}Ca_{0.5-x}Sr_xMnO_3$ system. Similar behavior has been observed in polycrystalline $La_{1-x-y}R_yCa_xMnO_{3-\delta}$ manganites, wherein the intensity and position of the absorption peak are influenced by the modification in local lattice distortions as a function of doping [15].

Thus, with increasing Sr doping (increasing A-site ionic radii $< r_A >$ and disorder σ^2) the stretching mode peak is weakened and delocalization tendencies are favored due to increase in $< Mn - O - Mn >$ bond angles towards 180° and therefore enhancing the one electron bandwidth. These structural modification leads to collapse of insulating gap and favor hopping and therefore result in charge delocalization. Effect similar to internal pressure (caused by increasing $< r_A >$) has been achieved on application of external pressure [22]. Previous pressure dependent infrared absorption studies at room temperature on $La_{0.75}Ca_{0.25}MnO_3$ system reveals reduction in optical band gap as pressure is increased [16, 26, 36].

4. Conclusion

We have investigated the half doped $La_{0.5}Ca_{0.5-x}Sr_xMnO_3$ ($0.1 \leq x \leq 0.5$) manganites with different magnetic ground states by infrared absorption measurements. In samples with CE-type antiferromagnetic ground states with $x \leq 0.3$, the stretching mode vibration of MnO_6 octahedra at $\sim 615 - 620 cm^{-1}$ in addition to a mode at $\sim 510 - 525 cm^{-1}$ attributable to charge ordered phase is evident for these samples. The obtained values of insulating band gap $2\triangle(T)$ and effective number of charge carriers $n^*_{eff}(T)$ in x = 0.1 and 0.3 samples, exhibit decrease on lowering of temperature. At 100K, the values of $2\triangle(T)$ in x = 0.1 and 0.3 samples are $\sim$ 727(1) and 605(1)cm^{-1}, respectively. For Sr doping with $x \geq 0.4$, considerable weakening of stretching mode is seen, while shoulder ascribed to charge ordered state is absent.

References

[1] C. N. R. Rao and B. Raveau, Colossal Magnetoresistance, Charge Ordering, and Related Properties of Manganese Oxides World Scientific, 1998, Singapore.

[2] E. Dagotto, Nanoscale Phase Separation and Colossal Magnetoresistance, Springer Series in Solid State Physics Vol. 136 Springer, 2003, Berlin.

[3] J. B. Goodenough, in Handbook on the Physics and Chemistry of Rare Earth, edited by K. A. Gschneidner, Jr., J.-C. Bunzli, and V. K. Pecharsky Elsevier Science, Vol. 33, 2003, Amsterdam.

[4] Y. Tokura, Rep. Prog. Phys. 69, 797 (2006).

[5] A. J. Millis, P. B. Littlewood, and B. I. Shriaman, Phys. Rev. Lett. 74, 5144 (1995).

[6] D. Louca, T. Egami, E. L. Brosha, H. Roder, and A. R. Bishop, Phys. Rev. B 56, R8475 (1997).

[7] C. P. Adams, J. W. Lynn, Y. M. Mukovskii, A. A. Arsenov, and D. A. Shulyatev, Phys. Rev. Lett. 85, 3954 (2000).

[8] K. H. Kim, J. Y. Gu, H. S. Choi, G. W. Park, and T. W. Noh, Phys. Rev. Lett. 77, 1877 (1996).

[9] A. J. Millis, Nature (London) 392, 147 (1998).

[10] M. N. Iliev, M. V. Abrashev, H. G. Lee, V. N. Popov, Y. Y. Sun, C. Thomsen, R. L. Meng, and C. W. Chu, Phys. Rev. B 57, 2872 (1998).

[11] M. Rini, R. A. Tobey, N. Dean, J. Itatani, Y. Tomioka, Y. Tokura, R. W. Schoenlein, and A. Cavalleri, Nature 449, 72 (2007).

[12] E. G. Rini, Mala N. Rao, S. L. Chaplot, N. K. Gaur, and R. K. Singh, Phys. Rev. B 75, 214301 (2007).

[13] J. D. Lee and B. I. Min, Phys. Rev. B 55, 14713 (1997).

[14] J. D. Lee and B. I. Min, Phys. Rev. B 55, 12454 (1997).

[15] L. Kebin, L. Xijun, and Z. Kaigui, Z. Jingsheng and Z. Yuheng, J. Appl. Phys. 81, 6943 (1997).

[16] A. Sacchetti, M. C. Guidi, E. Arcangeletti, A. Nucara, P. Calvani, M. Piccinini, A. Marcelli, and P. Postorino, Phys. Rev. Lett. 96, 035503 (2006).

[17] P. Calvani, G. De Marzi, P. Dore, S. Lupi, P. Maselli, F. D'Amore, S. Gagliardi, and S.-W. Cheong, Phys. Rev. Lett. 81, 4504 (1998).

[18] P. G. Radaelli, D. E. Cox, M. Marezio and S. -W. Cheong, Phys. Rev. B 55, 3015 (1997).

[19] C. H. Chen and S. -W. Cheong, Phys. Rev. Lett. 76, 4042 (1996).

[20] I. Dhiman, A. Das, P. K. Mishra, and L. Panicker, Phys. Rev. B 77, 094440 (2008).

[21] I. Dhiman, A. Das, R. Mittal, Y. Su, A. Kumar, and A. Radulescu, Phys. Rev. B 81, 104423 (2010).

[22] I. Dhiman, Thierry Strässle, L. Keller, B. Padmanabhan, and A. Das, Phys. Rev. B 81, 104424 (2010).

[23] A. Paolone, P. Giura, P. Calvani, P. Dore, S. Lupi, and P. Maselli, Physica B 244, 33 (1998).

[24] I. S. Smirnova, Physica B 262, 247 (1999).

[25] A. Paolone, P. Roy, A. Pimenov, A. Loidl, O. K. Mel'nikov and A. Ya. Shapiro, Phys. Rev. B 61, 11255 (2000).

[26] A. Congeduti, P. Postorino, P. Dore, A. Nucara, S. Lupi, S. Mercone, P. Calvani, A. Kumar, and D. D. Sarma, Phys. Rev. B 63, 184410 (2001).

[27] V. TaPhuoc, R. Sopracase, G. Gruener, J. C. Soret, F. Gervais, A. Maignan, and C. Martin, Materials Science and Engineering B104, 131 (2003).

[28] M. Premila, T. N. Sairam, and C. S. Sundar, Current Science 88, 102 (2005).

[29] Z. M. Lu, J. R. Sun, Y. Zhao, S. T. Li, H. Y. Liu and Y. X. Li, J. Appl. Phys. 99, 08Q303 (2006).

[30] K. H. Kim, J. H. Jung, D. J. Eom, T. W. Noh, J. Yu, and E. J. Choi, Phys. Rev. Lett. 81, 4983 (1998).

[31] K. H. Kim, S. Lee, T. W. Noh, and S.-W. Cheong, Phys. Rev. Lett. 88, 167204 (2002).

[32] A. P. Litvinchuk, M. N. Iliev, M. Pissas, and C. W. Chu, Solid State Commun. 132, 309 (2004).

[33] H. J. Lee, K. H. Kim, M. W. Kim, T. W. Noh, B. G. Kim, T. Y. Koo, S.-W. Cheong, Y. J. Wang, and X. Wei, Phys. Rev. B 65, 115118 (2002).

[34] C. A. Perroni, V. Cataudella, G. De Filippis, G. Iadonisi, V. Marigliano Ramaglia, and F. Ventriglia, Phys. Rev. B 67, 094302 (2003).

[35] J. H. Jung, H. J. Lee, J. Yu, T. W. Noh, E. J. Choi, and Y. Moritomo, Phys. Rev. B 61, 14656 (2000).

[36] A. Sacchetti, P. Dorea, P. Postorinoa, and A. Congeduti, Journal of Physics and Chemistry of Solids 65, 1431 (2004).

List of Figures

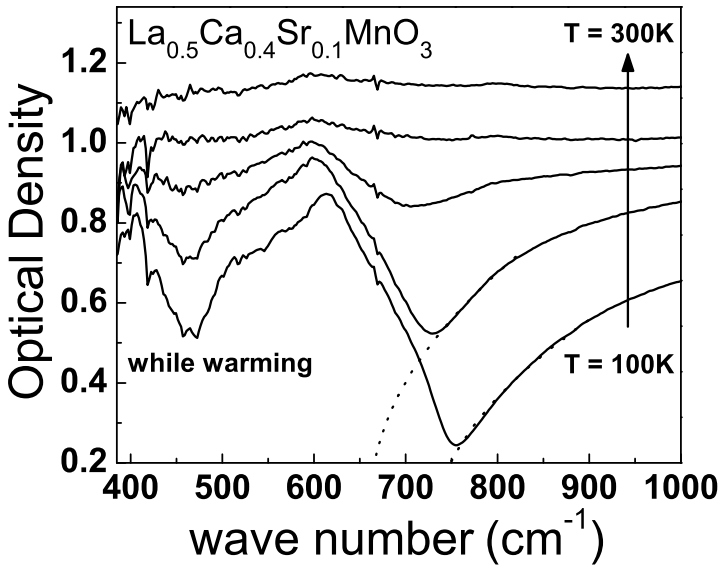

Figure 1: Optical density $O_d(\omega)$ for $La_{0.5}Ca_{0.4}Sr_{0.1}MnO_3$ (x = 0.1) sample at various temperatures between 100 to 300K. The dotted lines represent the extrapolation based of equation 1. Optical density patterns have been artificially shifted to enhance clarity.

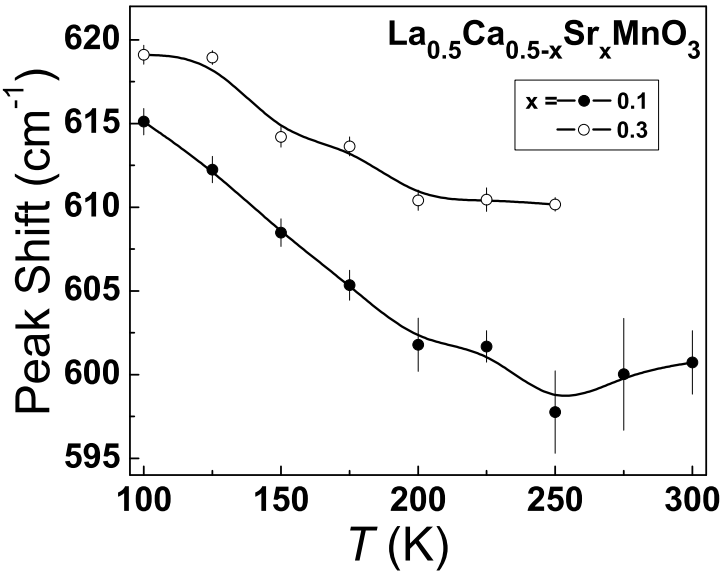

Figure 2: Frequency shift of the stretching mode peak at $\sim 600 - 620 cm^{-1}$ as a function of temperature for $La_{0.5}Ca_{0.5-x}Sr_xMnO_3$ (x = 0.1 and 0.3) samples.

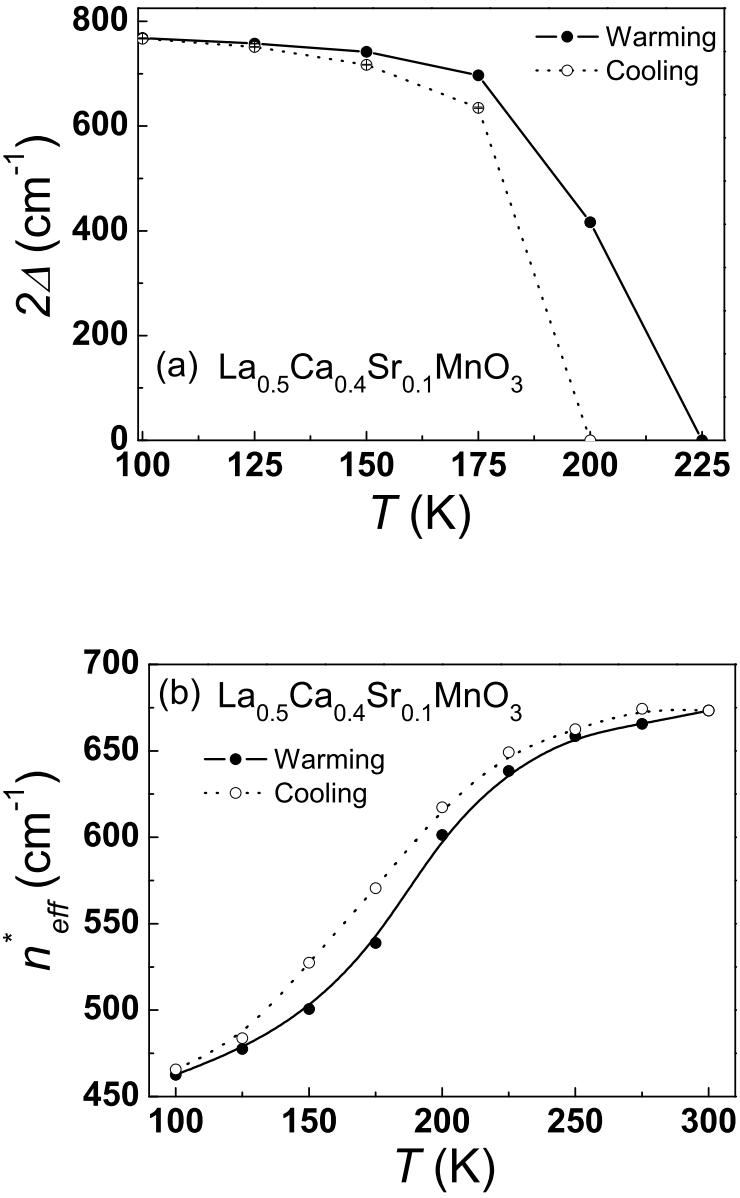

Figure 3: (a) the optical band gap (2Δ) and (b) effective number of carriers (n^*_{eff}) as a function of temperature for $La_{0.5}Ca_{0.4}Sr_{0.1}MnO_3$ sample for warming (solid lines and full circles) and cooling (dotted lines and open circles) cycles.

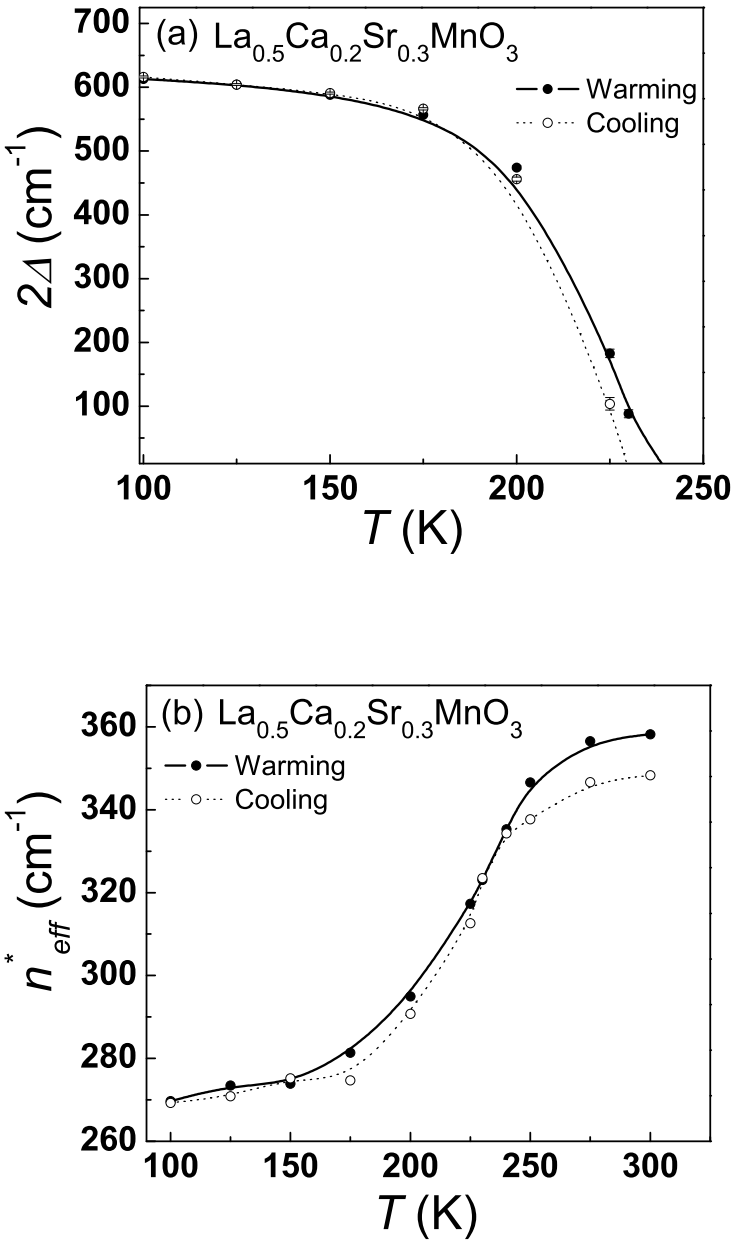

Figure 4: (a) the optical band gap (2Δ) and (b) effective number of carriers (n^*_{eff}) as a function of temperature for $La_{0.5}Ca_{0.2}Sr_{0.3}MnO_3$ sample for warming (solid lines and full circles) and cooling (dotted lines and open circles) cycles.

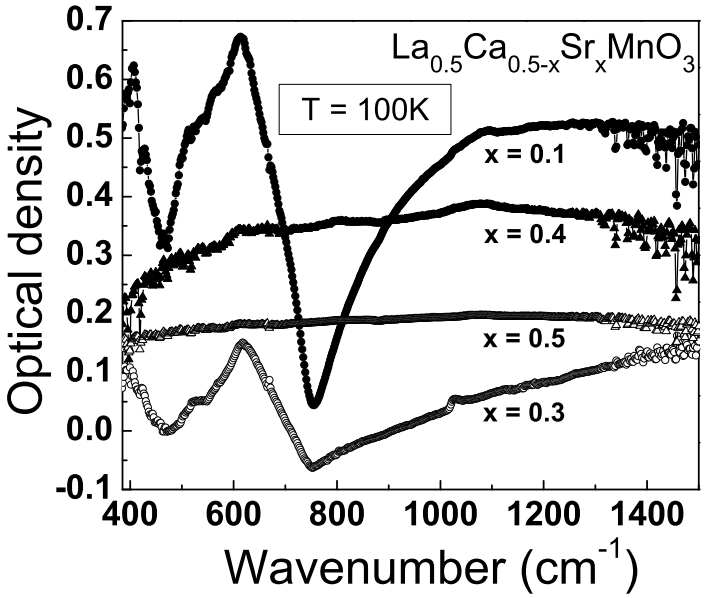

Figure 5: Infrared absorption spectra for $La_{0.5}Ca_{0.5-x}Sr_xMnO_3$ ($0.1 \leq$ x ≤ 0.5) series at 100K.